https://
doi.org/10.1080/17480272.2023.2289023

Coatings deposited by physical vapor deposition (PVD) on high-speed steel used in the processing of wood materials

Paweł Czarniak[a], Beata Kucharska[b], Karol Szymanowski[a], Corinne Nouveau[c], Peter Panjan[d], Krzysztof Kulikowski[b], Agata Roguska[e], Maksymilian Gloeh[a] and Jerzy Robert Sobiecki[b]

[a]Warsaw University of Live Sciences, Institute of Wood Sciences and Furniture, Department of Wood Mechanical Processing, Warsaw, Poland; [b]Warsaw University of Technology, Department of Material Engineering, Warsaw, Poland; [c]Institute of Technology, Department of Materials and Surface Engineering, Cluny, France; [d]Jozef Stefan Institute, Ljubljana, Slowenia; [e]Institute of Physical Chemistry, Polish Academy of Sciences, Warsaw, Poland

ABSTRACT

In this study the use of AlTiN/aCN, TiAlN/TiN and three types of CrAlN/CrN coatings deposited on HSS steel was investigated. These protective coatings were prepared using PVD (physical vapor deposition) method. The objective of this study was to compare the microstructure, chemical composition and properties of Cr, Al or Ti based coatings deposited on a substrate made of high-speed steel HSS. The thicknesses of coatings based on titanium were approx. 4 µm, and those based on chromium were less than 1 µm. The morphology and chemical composition were studied using scanning electron microscopy (SEM) and X-ray dispersion spectroscopy (EDX). The X-ray photoelectron spectroscopy (XPS) method was applied. The adhesion was evaluated by scratch test. Nanohardness and durability tests of uncoated and coated knifes were performed. It was found that the knifes made of HSS covered with two-layer TiAlN/aCN coating exhibited the best durability characteristic. Coatings containing chromium were less durable due to their small thickness. The highest nanohardness was found in the AlTiN/TiN coating due to its multi-layer nature. The nanohardness of the other coatings is comparable but more than two times lower compared to the multilayer AlTiN/TiN nanocoating.

KEYWORDS

PVD method; AlTiN/aCN; TiAlN/TiN; CrAlN/CrN; HSS steel; tool durability tests

Introduction

One of the most commonly used tool materials in the wood industry when processing solid wood is high-speed steel. The advantages of this material are its low price and the possibility of making special knives (up to 4 m long) with a very small blade angle, i.e. 16–20°, which ensure good surface roughness. Numerous efforts have been made to increase the tool life and cutting performance of tools made of HSS. Layers produced using low-temperature glow nitriding are widespread by Rudnicki et al. (1998), Beer et al. (2005). In the work of Beer et al. (2003), hard layers of chromium nitrides were produced on the nitrided substrate. Improving the durability of the tools. CrN layers (10% N_2 in the gas mixture) with a cubic structure and Cr_2N layers (above 20% N_2 in the gas mixture) with a hexagonal structure were also used by Djouadi et al. (2000). In the work of Warcholinski et al. (2011) described single-layer coatings as well as alternating multi-layer CrN and Cr_2N coatings. The substrate was HS 6-5-2 high-speed steel.

The addition of carbon to chromium coatings was described in the work of Gilewicz et al. (2010). In this work, as well as in others such as Polcar et al. (2005, 2010), a beneficial effect of the carbon content on the behavior of CrN-type coatings was demonstrated, allowing for operation at temperatures up to 400°C. Carbon-modified Cr-based coatings (CrN-CrCN) have been introduced into practice in two Polish tool factories FABA Baboszewo and GOPOL. A gradient multilayer structure was proposed. The content of individual CrN and CrCN layers changed gradually. The carbon content in the analyzed coatings was about 10%, and they were deposited on HS 6-5-2 steel by cathodic arc evaporation.

Multi-layer coatings based on CrN, CrCN applied to HSS high-speed steel by the PVD method can be improved by introducing an anti-wear DLC coating using the RF PACVD method. Within the DLC layers, a-C or ta-C can be distinguished. The differences consist mainly of the different content of sp3 bonds. According to Vetter (2014), ta-C carbon has 50% sp^3 bonds and a hardness of at least 50 GPa.

Among many works analysing the properties of DLC coatings applied to knives made of high-speed steel, the work of Faga (2006) deserves attention, in which the suitability of DLC layers on HSS 18 high-speed steel and AS 90CMV8 alloy steel produced by the RF PACVD method was verified. A very hard ta-C layer was the subject of the work of Gilewicz et al. (2013). Chemical analysis showed that the source of its high hardness is the presence of sp^3 bonds estimated at about 40%. CrCN/CrN coatings produced on HSS 18-0-1 blades improved tool life twice during the processing of seasoned dry pine timber, and the use of a ta-C surface layer on the CrCN/CrN surface additionally increased tool life by 15%.

Obtaining the ta-C form is associated with great technological difficulties. Therefore, Pancielejko et al. (2012) proposed hybrid methods of deposition of carbon layers enabling the

CONTACT Paweł Czarniak pawel_czarniak@sggw.edu.pl Warsaw University of Live Sciences, Institute of Wood Sciences and Furniture, Department of Wood Mechanical Processing, Nowoursynowska 159 str., 02-787 Warsaw, Poland

production of metal carbides by injection of a reactive gas such as acetylene. This leads to the formation of a nanostructured carbide coating with a ta-C surface layer. The increase in tool life of the carbide tools was 300% when milling a floorboard. Unfortunately, according Pancielejko et al. (2013) in the case of the HSS substrate, the durability increased by only 30%.

Aluminum is very often introduced into the structure of coatings on cutting tools. Warcholiński et al. (2011) confirmed the advantages of the addition of Al in the layer deposited on HSS 6-5-2 steel. The authors investigated single-layer TiN, TiAlN, and multi-layer TiAlN/TiN coatings. Seven layers, each 400 nm thick, were deposited in this work. According to Kot et al. (2008) this thickness value provides the best mechanical properties, the high hardness, high Young's modulus, and the good adhesion. The thickness ratio of the two layers was 1:1 and the total thickness of the coating was 3 μm. The addition of aluminum in the TiAlN coating increases hardness, abrasion resistance, and oxidation up to 800°C, as showed Benlatreche et al. (2009).

Based on the presented literature, it seems purposeful to compare the properties of selected coatings dedicated to the treatment of wood materials based on both Cr and Al. or Ti deposited on a substrate made of high-speed steel HSS.

Analysing the available literature, it can be concluded that despite the dynamic development of tools for processing wood materials based on WC-Co sintered carbides, HSS tools still play an important role in the wood industry. This type of tools are especially used when processing solid wood. Moreover, two main trends can be observed in tool coating technology, which differs in the type of elements used. The first type of coatings contains chromium compounds, and the second type contains titanium and aluminum compounds. There is no comparison in the literature of the operational properties of these types of coatings in difficult conditions on chipboard. Another significant breakthrough in these technologies is the use of innovative multi-layer and gradient coatings, in which varying the thickness of individual layers is intended to improve the properties of the coatings.

The aim of this work is to determine which group of coatings, i.e. those based on chromium or titanium/aluminum compounds, is characterized by better mechanical and operational properties when using an HSS substrate. Various types of coatings were used in the research in terms of chemical composition and their structure (single-layer, multi-layer, gradient) in order to compare their properties in the processing of wood materials.

1. Materials and methods

1.1. Coatings synthesis

The coatings AlTiN/TiN, aCN/TiAlN, CrN, M1 (CrN/CrAlN grad.), and M2 (CrN/AlCrN) were tested. AlTiN/TiN and aCN/TiAlN coatings were produced by the Josef Stefan Institute in Ljubljana and CrN, M1 (CrN/CrAlN grad.), and M2 (CrN/AlCrN) coatings by the Institute of Technology in Cluny. The substrate was HSS steel.

All coatings made by the Josef Stefan Institute were applied using the magnetron sputtering method on an industrial device CC800/9 (Cemecon, Würselen, Germany). The system in which the device was equipped consisted of four multi-part sources placed in one plane, placed in the corners of the chamber (dimensions 88 × 500 mm). In the case of the AlTiN/TiN multilayer coating, three-segmented AlTi sources and one source containing Ti were used alternately. On the other hand, the process of deposition of a two-layer aCN/TiAlN coating was carried out in two stages, i.e. first a segmented source of TiAl was used, and then graphite with a purity of 99.8%.

Prior to the application of the Slovenian coatings, the substrate was treated with detergents and ultrasound, then immersed in deionized water and dried in hot air. In the first stage, the process of medium-frequency ion etching was carried out using a voltage of 650 V, a gas mixture flow (Ar ~120 sccm, krypton ~50 sccm), pressure 0.35 Pa, and a time of 45 min. In the presence of argon (120 sccm) and krypton (90 sccm), the inside of the chamber was cleaned (p = 0.43 Pa, voltage 170 V, t = 15 min). Initially, the chamber was heated to 450°C at a pressure of 0.004 Pa.

The coatings produced by the Institute of Technology were also obtained using magnetron sputtering (Kenosistec model KS40V-113K12). Square sources (406.4 mm × 127 mm × 6.35 mm) containing Cr (purity 99.95%) and Al (purity 99.5%) were placed side by side in the chamber. The substrate holders were on a double-rotation planetary carousel, similar to the Cemecon system in Ljubljana.

The distance between the sources and the rotating holder with the knives attached was 120 mm. The substrates were cleaned outside the chamber (ultrasonic bath in both acetone and ethanol after 10 min) and in the chamber (etching with argon flow of 150 sccm, voltage −700 V, pressure 0.7 Pa, and time 5 min). During the deposition, a gas mixture of Ar + N2 (99.99% purity) was used. Also, the sources placed in the chamber were purified (argon flow 100 sccm Ar, pressure 0.5 Pa, voltage applied to the source 340 V, time 10 min.). A detailed list of process parameters during the application of individual coatings is presented in Table 1.

1.2 The planned structure of the coatings

The total thickness of the TiN/AlTiN multilayer coating is planned to be about 4.5 μm. This coating consists of alternating nanolayers of TiN with a thickness of several nm and layers of AlTiN with a thickness of 20 nm. The near-surface layer consists of a layer of TiN lying at the very top with a thickness of 80 nm and a deeper layer of AlTiN with a thickness of 50 nm. The structure of the aCN/TiAlN coating was planned as a two-layer structure with a total thickness of 3.9 μm. The ratio between the thickness of the TiAlN layer and the a-CNx layer was to be 6:1.

The parameters of the processes in France have been selected to produce coatings with a thickness of approx. 2 μm. Coatings containing chromium compounds contain an intermediate layer containing pure chromium with a thickness of 200 nm, Polcar et al (2005). The coating marked as M1 is composed of 4 CrN/CrAlN pairs of decreasing thickness starting from the substrate to the near-surface layer. The thickness of each CrN/CrAlN pair should be 1000, 500, 250, and 200 nm, respectively.

Table 1. Parameters of the coating application process.

Coating		*AlTiN/TiN*	*aCN/TiAlN*	*CrN*	*M1*	*M2*
Argon flow (sccm)	AlTi/Ti	135	-			
	TiAl	-	100			
	C	-	150			
	Cr			100	92	100
	CrN			60	68.6	60
	AlCrN			–	–	60
	CrAlN			–	68.6	–
Nitrogen flow (sccm)		120	160 / 60	53	33.3	53
Working pressure (Pa)		0.64	0.6 / 0.4	0.5		
Power	AlTi/Ti	9500	–			
	TiAl	–	9500 / 4000			
Power on chromium target (W)	Cr			1500		
	CrN			1500		
	AlCrN			–	–	500
	CrAlN			–	1500	–
Power applied on the aluminum target (W)				0	1000	1500
Deposition time min	AlTi / Ti	145	–			
	TiAl / C	–	210 / 150			
	Cr			15	10	15
	CrN			360	60/30/15/12*	25 × 8
	AlCrN			–	–	40 × 8
	CrAlN			–	60/30/15/12*	–
Deposition temperature (°C)		450	450	300		
Substrate bias voltage (V)	AlTi / Ti	90	–			
	TiAl / C	–	90 / 80			
	Cr			500		
	CrN			500		
	AlCrN			–	–	250
	CrAlN			–	500	–

* The deposition time presented for M1 is the deposition time for each monolayer from the thicker to the thinner.

The coating marked as M2 should consist of 8 CrN/AlCrN pairs, with a thickness of 375 nm each. A list of all the most important properties of this type of coating can be found in Zhang (2022). Figure 1 shows the planned structure of individual Slovenian and French coatings.

1.3 Morphology, chemical composition, surface roughness and thickness

The analysis of the morphology, surface topography, and chemical composition of the coatings was carried out using a Hitachi SU-70 scanning electron microscope (SEM) equipped with the Energy Dispersive X-ray Spectroscopy (EDS) microanalysis system. Surface roughness measurements were carried out on the surface of the specimens using a surface roughness tester (Mitutoyo, Japan). The pin tip was slid along the coated and uncoated surfaces with a 0.8 mm cut-off length. The thickness of the coatings was determined using the ball wear culotester (Culotester, Radom, Polska). Culotester is a test system for the precise identification of microstructures in multilayer coatings and for observation of coating-substrate contact areas. The applications of this device include, among others, coatings applied by CVD and PVD techniques in the range of coating thicknesses of 1–20 µm with the geometric magnification of the coating thickness up to 45 times. The ball used was made of 100Cr6 steel, its diameter was 30 mm, and its rotational speed was 7.5 rpm.

1.4 XPS studies

The X-ray photoelectron spectroscopy (XPS) measurements of the coatings were performed with a Microlab350 (Thermo Electron, Waltham, USA) using AlKα non-monochromatic radiation (1486.6 eV) as a source, with a maximum resolution of 0.83 eV. The survey and high-resolution spectra were recorded at a constant pass energy of 100 and 40 eV, respectively. Avantage Surface Chemical Analysis software (ThermoFisher Scientific, Waltham, USA) was utilized to evaluate the XPS data. Deconvolution of the spectra was performed using a smart-type background and a Gaussian peak shape with a 35% Lorentzian character. The binding energies (BEs) of all detected elements were corrected with respect to the BE of C 1 s peak at 284.8 eV.

1.5 Durability tests, nanohardness and adhesion

During the durability tests, the Busellato JET Machining Centre was used, which is equipped with the laboratory at the Warsaw University of Life Sciences. Knives made of HSS high-speed steel with catalogue number 630,000 were used for the tests. The manufacturer of the tools was ITA TOOL (see references). The dimensions of the knives were 50 × 32 × 4 mm. For blunting, a standard MDF board with a thickness of 16 mm. The assumed rotational speed of the tool was 12,000 RPM, which at the feed rate of 1.8 m/min gave the feed per tooth $\Delta z = 0.15$ mm. The thickness of the cut layer was 5 mm. The tests included 7 blades in each variant. Due to the large differences in the precise setting of individual knives in the head, the so-called blind knife with recessed cutting edge. Each blunting cycle covered a travel distance of 0.7 m. After the end of each cycle, the wear indicator (VB max) was measured on a workshop microscope. The blunting process for each of the blades was interrupted after the blade reached the assumed blunting criterion VB

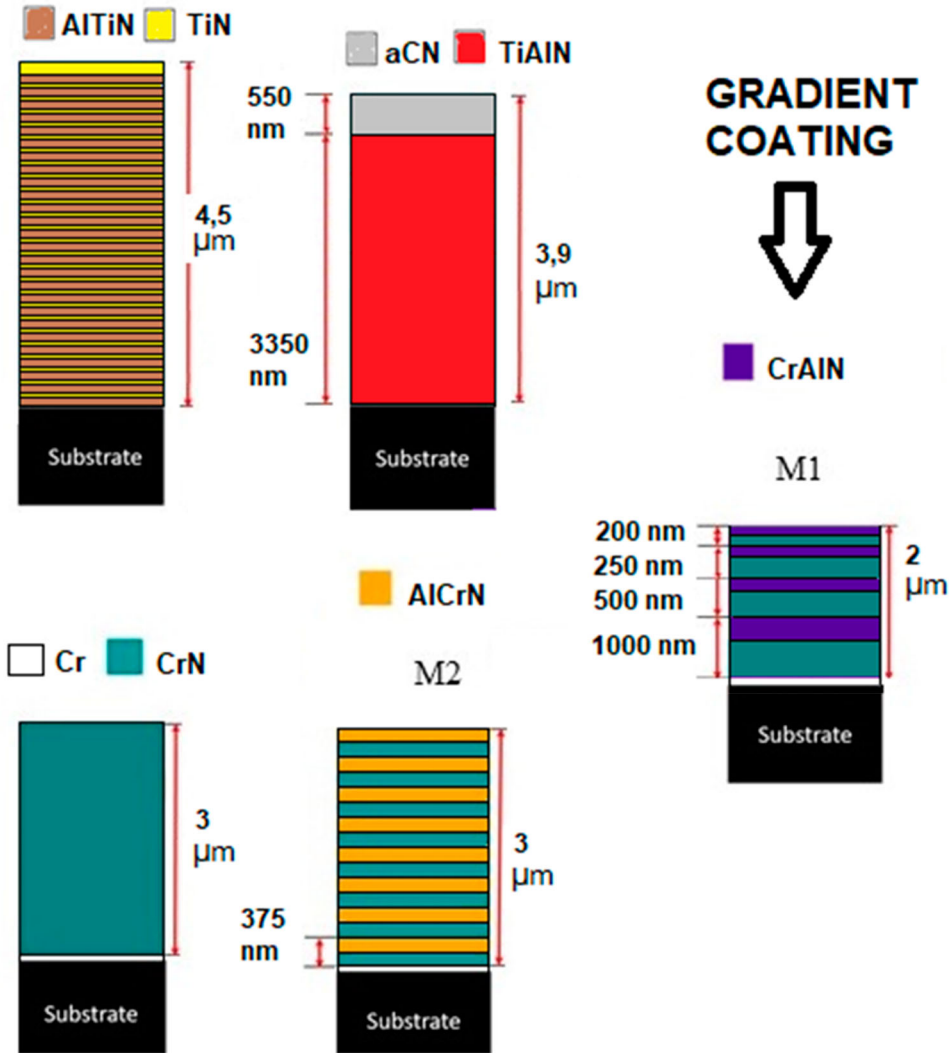

Figure 1. The planned structure of the coatings.

max = 0.3 mm. Figure 2 shows the machining diagram and the methodology for calculating the cutting path based on the recorded tool travel path. Then, the feed path was converted to the cutting path according to the following formula (Figure 2). The results of the service life were determined on the basis of the cutting path travelled by the blades to achieve the blunting criterion VB max = 0.3 mm.

Coating hardness was determined by nanoindentation using a NanoTest Vantage (Micromaterials Ltd., Wrexham, UK) with a Berkovich diamond indenter. The average hardness was obtained from a minimum of 8 impressions. The indenting load was 20 mN, and the time of loading and unloading was 10 s. The parameters that were adopted during the nanohardness test are listed in Table 2.

The adhesion of the coatings to the substrate was analysed using a scratch tester (CSM Instruments RST, USA), in which the load on the indenter was changed from 1 to 50 N over a distance of 8 mm. The adhesion of the coatings was assessed on the basis of the values of critical forces Lc2, determined by means of acoustic emission measurements and images of cracks after the scratch test.

2. Results and discussion

2.1. SEM and EDS analysis

The SEM micrographs (Figure 3) show significant differences in the homogeneity of the structure of the analysed coatings. The surface of the AlTiN/TiN coating visible in Figure 3 indicates the presence of fine precipitations in the form of globules. The surface morphology does not reflect the topography of the substrate. However, its structure seems to be uniform, without clear traces of finishing operations carried out on the tool before applying the coating, which may leave delicate furrows. The aCN/TiAlN coating is devoid of the aforementioned globules, but it can be seen that it reflects the topography of the substrate used. Coatings based on chromium compounds look much worse. They have a completely different morphology. Deep grooves with jagged and uneven edges are visible in the CrN coating. The grooves visible in the CrN/AlCrN multilayer coating are smaller. However, in the case of the CrN/AlCrN gradient coating, the grooves are very clear and wide.

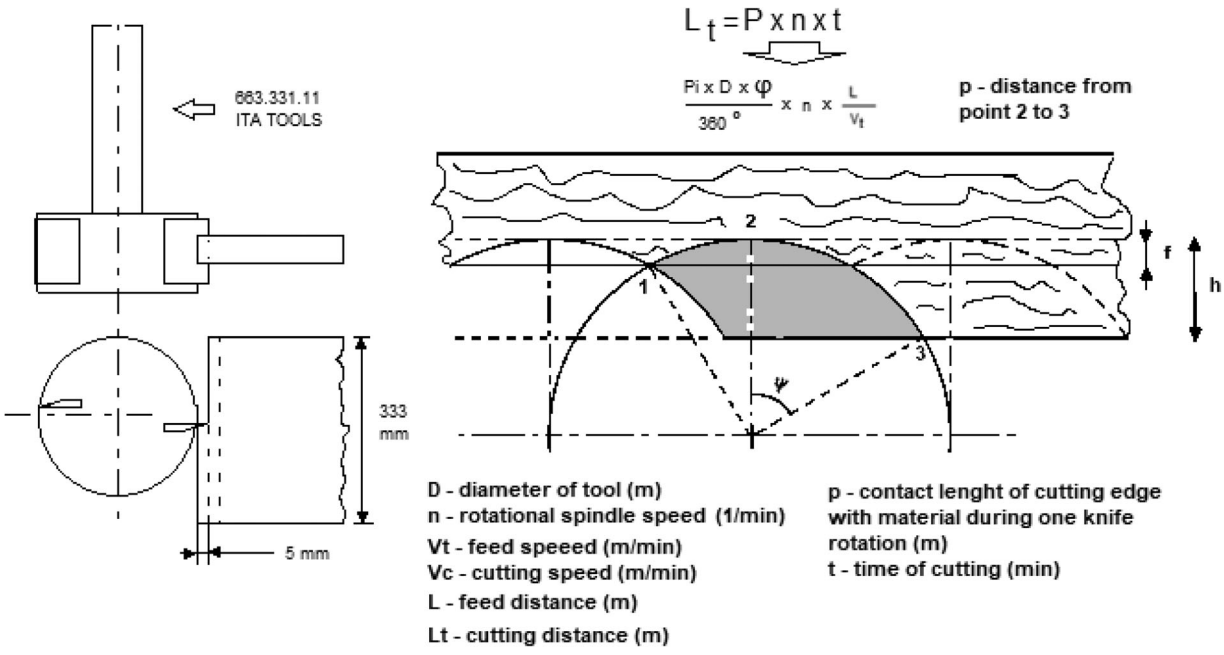

Figure 2. Scheme of blunting process and methodology of cutting distance calculation Lt.

Table 2. List of parameters during nanohardness tests.

Max. load pr (mN)	Loading time (s)	Unloading time (s)	Dwell period (s)
20	10	10	5

The atomic share of individual elements in the produced coatings is shown in Table 3. The results confirm the presence of the basic elements included in the analyzed coatings, such as, for example, C in the aCN/TiAlN two-layer coating. A greater share of Al in the AlTiN/TiN multilayer coating is also visible. On the other hand, the presence of Fe in chromium-containing coatings is caused by their too-small thickness. In the CrN/CrAlN gradient coating, even a 30% Fe share was observed. The penetration depth of the beam during the EDS test is approx. 2 µm, which indicates a lower than-assumed thickness of these coatings.

2.2. XPS analysis

XPS investigations allow the estimation of the chemical composition and the chemical environments of the elements present at the topmost surface. The coating's surface was analysed before and after an argon ions sputtering cleaning procedure. The initial surfaces were strongly contaminated and oxidized in all cases. Thus, they were analyzed after 3 min of argon ion etching to partially remove the top contaminant layer. After Ar^+ sputtering, a substantial decrease of carbon content (except aCN/TiAlN coating, for which the carbon content has

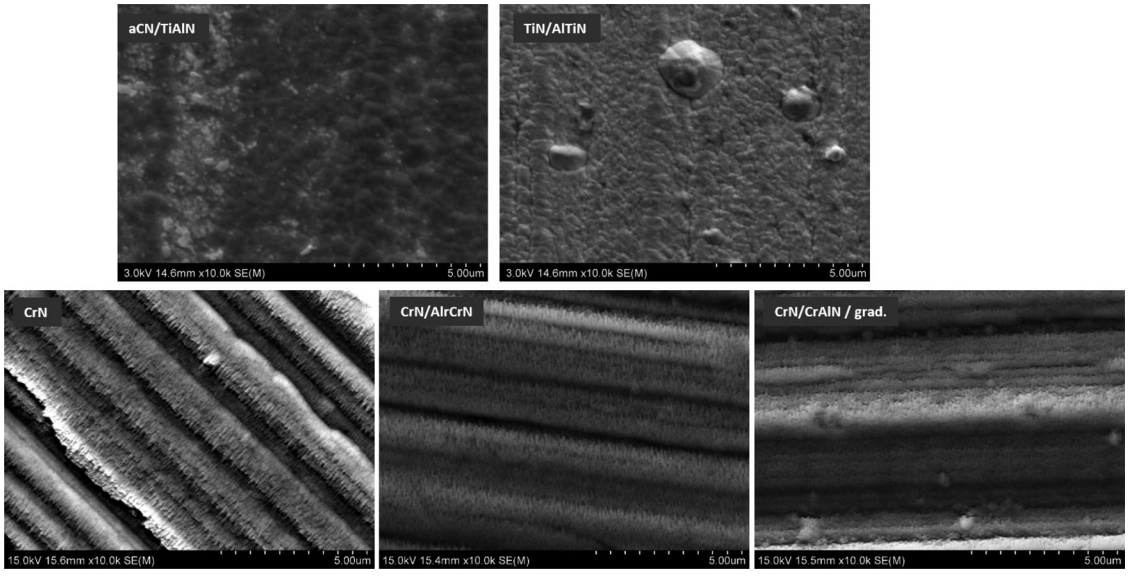

Figure 3. SEM micrographs of the analysed coatings.

Table 3. Chemical composition of the tested coatings obtained from EDS measurements.

Specimen	Chemical composition (at.%)						
	C	N	Cr	Al	Ti	O	Fe
TiN/AlTiN	6.2	30.1	–	39.8	23.8	–	–
aCN/TiAlN	64.3	10.7	–	11.9	13.2	–	–
CrN	8.4	30.4	43.3	–	–	7.2	10.7
CrN/AlCrN Multilayer	8.8	30.9	39.1	4.1	–	6.3	10.8
CrN/CrAlN gradient	8.9	28.5	33.5	3.7	–	6.3	19.1

slightly increased after Ar^+ ion sputtering) and higher intensity of N1s, Al2p, Ti2p and Cr2p signals due to surface cleaning were noticed. However, the carbonaceous contamination was not removed completely upon Ar^+ sputtering as the carbon is still present at the tested surfaces. Longer time of ion sputtering might remove the surface contamination completely but such a procedure produces chemical reduction, atomic mixing, preferential sputtering, and other effects that modify the surface. Except the constituent elements of the coatings the small amount of iron (0.7–2.7 at.%) was detected for all samples under investigation. The chemical composition of the tested coatings after Ar^+ ion etching obtained from XPS measurements is presented in Table 4.

XPS is a highly sensitive surface analysis method that probes approximately the top 10 nm of a film. The presence of Al at the surface of TiN/AlTiN coating indicates that the topmost TiN layer is much thinner than planned 80 nm and do not exceed several nanometers. The deconvoluted Ti2p, Al2p and N1s XPS spectra are presented in Figure 4a–c. The Ti2p spectrum split into the $Ti2p_{3/2}$ and $Ti2p_{1/2}$ components due to the spin–orbit interaction. The $Ti2p_{3/2}$ peak is resolved into three components with binding energies of 455.6, 457.3 and 458.8 eV, corresponding to the Ti-N bonds, Ti-O bonds in TiO2 and Ti-O bonds in titanium oxynitride as described in work of Obrasov et al. (2017) and Kucharska et al. (2022). The Al2p spectrum exhibits two components with binding energies of 73.6 and 74.7 eV, which can be attributed to Al–O bonds in Al_2O_3 or aluminum oxidenitride and Al-N bonds in aluminum nitride, respectively in work of Wang et al. (2011), Obrasov et al. (2017) and Kucharska et al. (2022). The N1s displays three components at 396.6, 397.8 and 399.3 eV. The main component with higher intensity centred at 396.6 eV can be ascribed to N bonded to metal (Ti and/or Al) in metal nitride, Jaeger and patsheider (2012). It is worth mentioning here, that the binding energies of N1s component originating from N bonded to specific metal in metal nitrides have been reported to lie between 396.5 and 397.7 eV (Wagner et al. 2012). Such a narrow range of energies makes unambiguous bonding structure assignment extremely cumbersome, if not impossible. Thus due to the very close position of N1s for pure TiN and AlN, these bonding states are not distinguished in the present study. The second component centered at 398.1 eV may be ascribed to N bonded to O in the metal nitride, while the weak component at 399.8 eV to N-O bond, where N is in different oxidation state as showed Wang et al. (2011), Jaeger and patsheider (2012) and Hsu and Lin (2020). Correspondingly, three different components were resolved in the O1s spectrum: O bonded to metal (component centered at 531.2 eV) and O bonded to N (components centred at 532.5 and 534.1 eV, respectively (Wang et al. 2011, Jaeger and patsheider 2012).

Table 4. Chemical composition of the tested coatings after Ar + ion etching obtained from XPS measurements.

Specimen	Chemical composition (at.%)						
	C	N	Cr	Al	Ti	O	Fe
TiN/AlTiN	18.2	21.9	–	33.9	6.8	18.3	0.9
aCN/TiAlN	79.0	13.2	–	–	–	6.7	1.2
CrN	35.8	19.0	19.1	–	–	23.5	2.7
CrN/AlCrN multilayer	30.1	9.9	16.5	6.3	–	35.5	1.7
CrN/CrAlN gradient	30.4	11.7	19.5	6.9	–	31.3	0.7

4The N and C content for aCN/TiAlN coating is found to be 13.2 and 79.0 at.%, respectively. The N/C ratio equals to 0.17. The content of oxygen does not exceed 7 at.% mainly due to contribution from metallic (iron) oxide compounds and adventitious surface contamination. The deconvoluted C1s and N1s spectra for aCN/TiAlN coating are shown in Figure 4d and e, respectively. The C1s spectrum exhibits four components at 284.8, 286.0, 287.5 and 289.2 eV. The main component centred at 284.8 eV is attributed to C atoms solely bonded to carbon neighbors, as in graphite or amorphous carbon, Hellgren et al. (2005). Due to the higher electronegativity of nitrogen, carbon bonded to nitrogen is expected to shift to higher values of the binding energy. Thus, the components centered at 286.0 and 287.5 eV can be attributed to various C–N bonds (carbon bonded to one and two nitrogen atoms, respectively). A weak component at 289.2 eV may be attributed to CO bonds due to adventitious surface contamination. The N1s spectrum exhibits three components centred at 398.9, 400.6 and 402.8 eV. The lowest N component is typically assigned either to N bonded to two C atoms as in pyridine, or N in a more tetrahedral environment, i.e. N bonded solely to sp^3-coordinated C (Rodil and Muhl 2004, Wicher et al. 2021), whereas higher binding energies may be associated with Nsp^2-C bonds or with the substitutional nitrogen in a graphite sheet (Rodil and Muhl 2004, Wicher et al. 2021). A tail at high binding energy (402.3 eV) is typically attributed N bounded to O, Bertoti and Mohai (2015). It has to be emphasized, however, that, the exact interpretations of the C1s and N1s components of carbon nitride coatings are controversial due to rather complex chemistry of CN compounds with rather limited chemical shifts in the 1–2 eV range for both elements.

The deconvoluted high-resolution XPS spectra for the constituent elements of the CrN-based coatings (deposited in France) are presented in Figure 4f–m. The Cr2p XPS spectra display characteristic spin–orbit splitting ($2p_{3/2}$ versus $2p_{1/2}$). The components at low binding energy of about 575 eV (low oxidation state) can be described as chromium-nitrogen (Cr–N) bonding as it displays metallic behavior according to Zeng et al. (2022). The origin of spectral features at higher binding energies suggested the formation of chromium oxynitrides (576.8–577.4 eV) or chromium oxides (579.7–580.1 eV) arising from spontaneous surface oxidation. The new signal at about 574 eV, which appeared for M1 and M2 coatings, corresponds

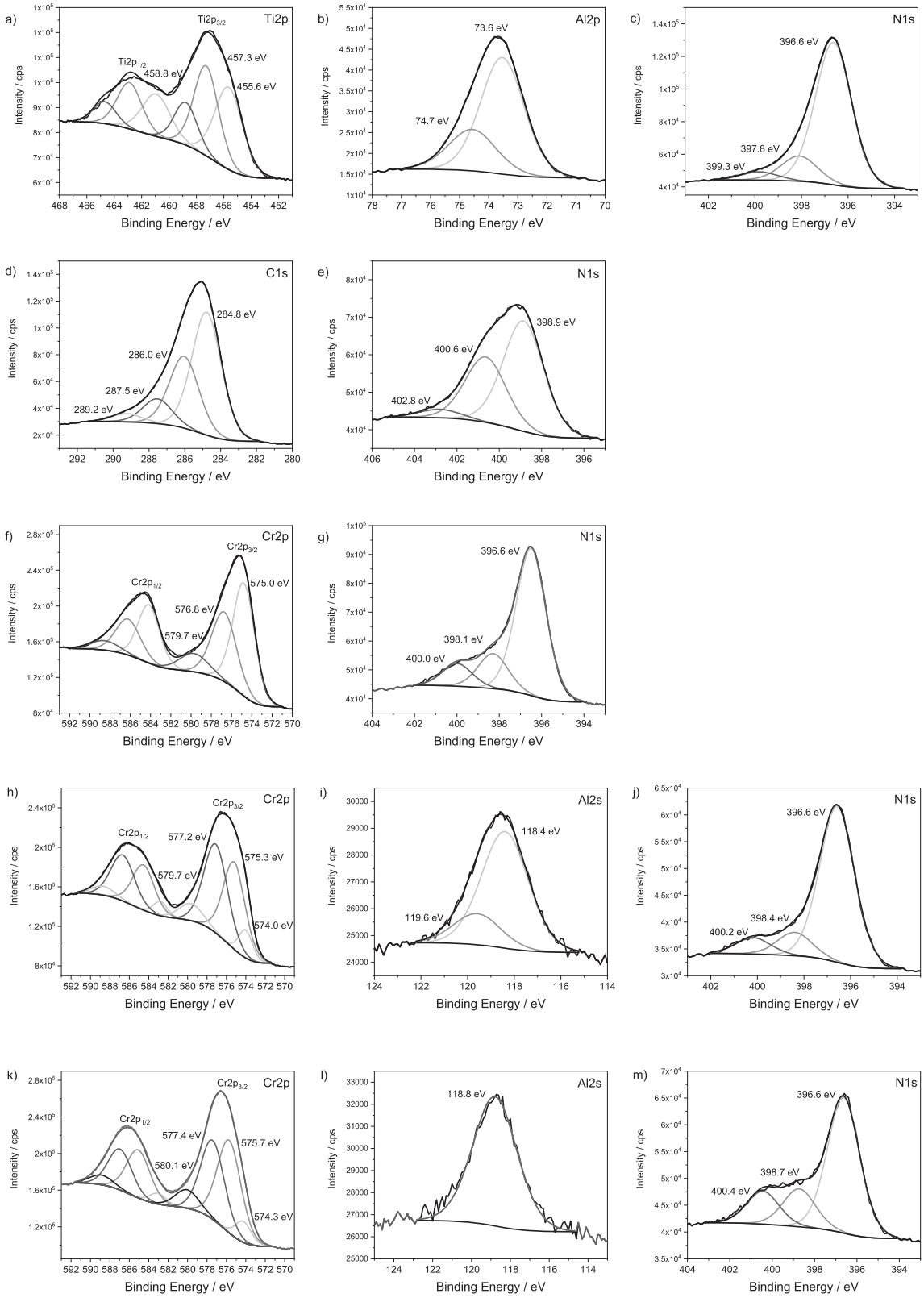

Figure 4. The high resolution XPS spectra measured for the tested coatings: (a–c) AlTiN/TiN, (d–e) aCN/TiAlN, (f–g) CrN, (h–k) CrN/CrAlN, and (l–m) CrN/AlCrN.

to chromium in metallic sate. The N1s spectra for all CrN-based coatings revealed the presence of a high intensity component characteristic to nitrogen in metal nitride (CrN or/and AlN) centered at 396.6 eV along with two weak components at a higher binding energies of about 398 and 400 eV, which may be attributed to N bonded to O species with different oxidation state of N, further indicating the formation of oxynitrides as noticed by Wang et al. (2011), Jaeger and patsheider (2012) and Hsu and Lin (2020). Due to the overlapping of Al2p and Cr3s XPS signals, for the analysis of M1 and M2 coatings Al2s

Table 5. Coating thicknesses and Ra/thickness ratio.

Type of coating	Thickness (µm)	Ratio Ra/thickness
AlTiN/TiN	3.50	0.14
aCN/TiAlN	4.20	0.09
CrN	0.50	0.50
CrN/AlCrN	0.59	0.62
CrN/CrAlN / gradient	0.54	0.37

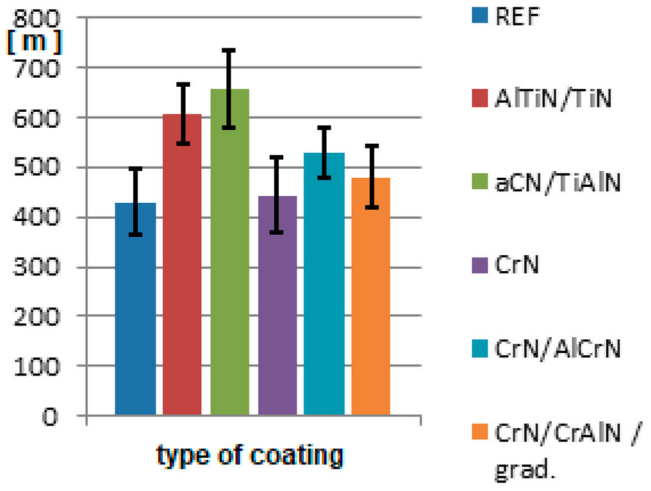

Figure 5. Results of durability tests.

signal was taken into consideration. The Al3s spectrum measured for CrN/CrAlN (M1) coating exhibits two components. The main component centered at 118.4 eV may be attributed to the Al-N bond while the weak component at 119.6 eV corresponds to Al–O bond, respectively (Wagner et al. 2012). The Al2s spectrum for CrN/AlCrN (M2) coating is composed from one component centered at 118.8 eV assigned to AlN. In summary, the comprehensive XPS analysis revealed that M1 and M2 coatings exhibit a similar topmost surface chemical composition with an chromium oxide layer on the parent nitride and likely with an interfacial layer of oxynitride.

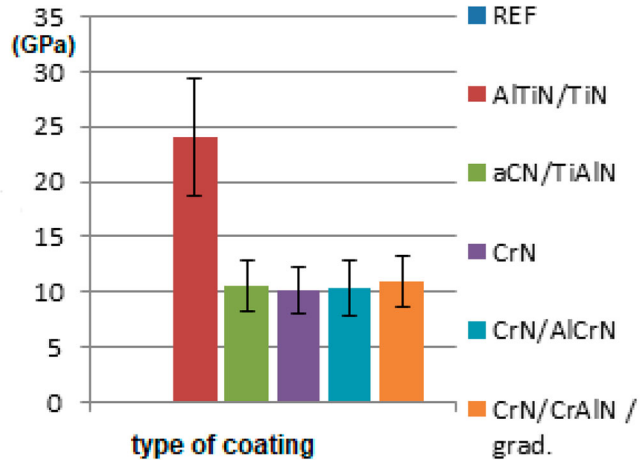

Figure 6. Nanohardness results.

2.3. Surface roughness and thickness of the coatings

The thickness of the coatings was verified using a bullet tester. The test results are summarized in Table 5.

Analysis of the thickness results confirms that the coatings based on chromium compounds are very thin. The conclusion is that the deposition times of the coatings produced in the Cluny laboratory were incorrectly selected for this type of substrate. It is worth noting that the Ra roughness index for coatings containing chromium compounds is close to the thickness obtained in tests. This phenomenon is particularly visible in the case of the CrN/CrAlN multilayer coating, where the Ra roughness index was about 0.38 µm, while the thickness of the said coating is only about 20% larger (about 0.5 µm). Taking into account the coatings based on Al and C, it can be seen that these differences are much greater. Table 5 shows the ratio of surface roughness (Ra) to thickness. The above list shows that even for the coating with the highest roughness, i.e. the AlTiN/TiN multilayer nanocoating, its thickness is about 7 times greater (3.5 µm vs. 0.5 µm)

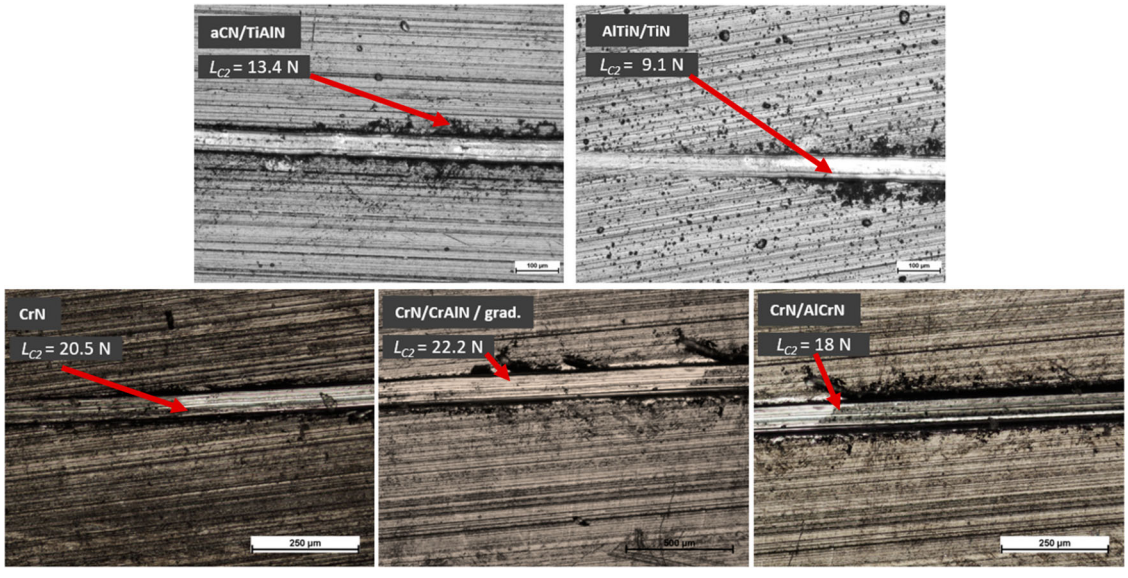

Figure 7. Scratch test results.

than the surface roughness determined by the Ra index, and in the case of the aCN/TiAlN coating even by about 12x larger (4.2 µm vs. 0.35 µm).

2.4 Durability tests, nanohardness and scratch tests analysis

The drawings showing the cutting path show much better durability results for Al and Ti-based coatings. Coatings containing chromium turned out to be definitely less durable due to their small thickness. The use of lower temperatures and too high polarization of the substrate resulted in the formation of coatings with a very thin thickness of several hundred nm. The etching parameters of the substrate before the formation of chromium-containing coatings were also not very well matched to the etching used in Ljubljana, because the increase in the gas flow, polarization voltage, and, above all, pressure in the chamber caused a significant expansion of the substrate surface, which is clearly visible in Figure 3. Results of durability tests are presernted in Figure 5.

The highest nanohardness was characteristic of the AlTiN/TiN coating due to its multi-layer nature. The nanohardness of the other coatings is comparable, but more than 2 x lower compared to the multilayer AlTiN/TiN nanocoating as shown in Figure 6.

Very good results for the aCN/TiAlN coating obtained in the durability test may indicate a positive effect of a thin near-surface layer of amorphous carbon. In adhesion tests during the scratch test of this coating, the friction coefficient reaches its maximum value of 0.6 only at a force of 20 N, and not at a force of 10 N, as is the case with the AlTiN/TiN coating. Tests of adhesion of coatings to the substrate show that thin coatings containing chromium have better adhesion to the substrate than thicker coatings based on Al and Ti. The Lc2 force is about twice as high. The development of the topography of the substrates during the etching process (which resulted in a reduction in thickness) results in better anchoring of the coatings, which results in their greater adhesion to the steel substrate. However, due to the abrasive wear mechanism of the blades, dominating the processing of wood materials, the operational properties of this type of coating turned out to be poor. Coatings with a thin surface layer of carbon have better adhesion to the substrate than multilayer AlTiN/TiN coatings. This may be due to the lubricating properties of the outer carbon layer. Multilayer coatings are characterized by higher nanohardness, but worse adhesion to the substrate. Fragments of cracks with the value of the Lc2 force are shown in Figure 7.

3. Conclusions

Coatings based on titanium and aluminum compounds showed much better mechanical properties than those containing chromium compounds, which contributed to a significant increase in the durability of tools during operational tests.

Gradient coatings require further research to optimize the application process. In particular, focus should be on the optimal course of etching the substrate surface before applying the coating.

The use of lower temperatures and too high polarization of the substrate resulted in the formation of coatings with a very thin thickness of several hundred nm. The etching parameters of the substrate before the production of chromium-containing coatings were also not very well selected, because the increase in the gas flow, polarization voltage, and, above all, the pressure in the chamber caused a significant expansion of the substrate surface.

Disclosure statement

No potential conflict of interest was reported by the author(s).

References

Aouadi, K., 2018. Développement d'une nouvelle génération de revêtements ultra-durs. Etude de leur comportement tribologique et anticorrosive: PhD thesis, Ecole nationale supérieure d'arts et métiers – ENSAM, 2017. https://pastel.archives-ouvertes.fr/tel-01799066/document (accessed May 25, 2018).

Beer, P., et al., 2003. Modification by composite coatings of knives made of low alloy steel for wood machining purposes. *Surface and Coatings Technology*, 174-175, 434–439.

Beer, P., et al., 2005. Low temperature ion nitriding of the cutting knives made of HSS. *Surface and Coatings Technology*, 200 (1–4), 146–148.

Benlatrechea, Y., et al., 2009. Applications of CrAlN ternary system in wood machining of medium density fibreboard (MDF). *Wear*, 267, 1056–1061.

Bertóti, I., and Mohai, M., 2015. Surface modification of graphene and graphite by nitrogen plasma: Determination of chemical state alterations and assignments by quantitative X-ray photoelectron spectroscopy. *Carbon*, 84, 185–196.

Bouzakis, K.-D., et al., 2010. Adaption of graded Cr/CrN-interlayer thickness to cemented carbide substrates' roughness for improving the adhesion of HPPMS PVD films and the cutting performance. *Surface and Coatings Technology*, 205, 1564–1570.

Djouadi, M.A., et al., 2000. CrN hard coatings deposited with PVD method on tools for wood machining. *Surface and Coatings Technology*, 133-134, 478–483.

Faga, M.G., 2006. Innovative anti-wear coatings on cutting tools for wood machining. *Surface and Coatings Technology*, 201, 3002–3007.

Gilewicz, A., et al., 2010. Anti-wear multilayer coatings based on chromium nitride for wood machining tools. *Wear*, 270, 32–38.

Gilewicz, A., Warcholinski, B., and Szymanski, W., 2013. CrCN/CrN+ta-C multilayer coating for applications in wood processing. *Tribology International*, 57, 1–7.

Hellgren, N., et al., 2005. Electronic structure of carbon nitride thin films studied by X-ray spectroscopy techniques. *Thin Solid Films*, 471, 19–34.

Hsu, J.-C., and Lin, Y.-H., 2020. X-ray photoelectron spectroscopy analysis of nitrogen-doped TiO_2 films prepared by reactive-ion-beam sputtering with various NH_3/O_2 gas mixture ratios. *Coatings*, 10 (1), 47.

Jaeger, D., Patsheider, J., 2012. A complete and self-consistent evaluation of XPS spectra of TiN. *Journal of Electron Spectroscopy and Related Phenomena*, 185, 523–534.

Kot, M., et al., 2008. Effect of bilayer period on properties of Cr/CrN multilayer coatings produced by laser ablation. *Surface and Coatings Technology*, 202, 3501–3506.

Kucharska, B., et al., 2022. Comparison study of PVD coatings: TiN/AlTiN, TiN and TiAlSiN used in wood machining. *Materials*, 15.

Obrosov, A., et al., 2017. Xps and AFM investigations of Ti-Al-N coatings fabricated using DC magnetron sputtering at various nitrogen flow rates and deposition temperatures. *Metals*, 7 (2), 52. doi:10.3390/met7020052.

Pancielejko, M., et al., 2013. The influence of the MCVA deposition parameters on the structure and trybological properties of DLC coatings on woodworking HSS tool substrates. *Archives of Materials Science and Engineering*, 64, 160–167.

Pancielejko, M., Szymański, W., et al., 2012. The cutting properties and wear of the knives with DLC and W-DLC coatings, deposited by PVD methods, applied for wood and wood-based materials machining. *Archives of Materials Science and Engineering*, 58, 235–244.

Polcar, T., et al., 2010. Effects of carbon content on the high temperature friction and wear of chromium carbonitride coatings. *Tribology International*, 43, 1228–1233.

Polcar, T., Cvrček, L., and Široký, P., 2005. Tribological characteristics of CrCN coatings at elevated temperature. *Vacuum*, 80, 113–116.

Rodil, S.-E., Muhl., S., 2004. Bonding in amorphous carbon nitride. *Diamond and Related Materials*, 13, 1521–1531.

Rudnicki, J., Beer, P., and Sokołowska, A., 1998. Low-temperature ion nitriding used for improving the durability of the steel knives in the wood rotary peeling. *Surface and Coatings Technology*, 107 (1), 20–23.

Vetter, J., 2014. 60 years of DLC coatings: Historical highlights and technical review of cathodic arc processes to synthesize various DLC types, and their evolution for industrial applications. *Surface and Coatings Technology*, 257, 213–240.

Wagner, C.-D., et al., 2012. NIST Standard Reference Database 20, Version 4.1 (web version) (http://srdata.nist.gov/xps/).

Wang, P.-W., Hsu, J.-C., and Lin, Y.-H., 2011. Structural investigation of high-transmittance aluminum oxynitride films deposited by ion beam sputtering. *Surface and Interface Analysis*, 43, 1089–1094.

Warcholinski, B., 2011. Multilayer coatings on tools for woodworking. *Wear*, 271, 2812–2820.

Warcholinski, B., Gilewicz, A., and Ratajski, J., 2011. Cr2N/CrN multilayer coatings for wood machining tools. *Tribology International*, 44, 1076–1082.

Wicher, B., et al., 2021. Applications insight into the plasmochemical state and optical properties of amorphous CNx films deposited by gas injection magnetron sputtering method. *Applied Surface Science*, 565.

Zeng, R., et al., 2022. Nonprecious transition metal nitrides as efficient oxygen reduction electrocatalysts for alkaline fuel cells. *Science Advances*, eabj1584.

Zhang, Y., 2022. Tool materials development for improved performance of cutting tools in cryogenic machining of Aeronautic Alloy, PhD thesis, Ecole nationale supérieure d'arts et métiers – ENSAM, https://pastel.archives-ouvertes.fr/tel-03635214/documenthttps://api.ita.tools/Media/Default/Documents/5680077E.pdf.